scientific reports

Check for updates

OPEN

Molecular evolution and reassortment dynamics of *Orthohantavirus hantanense* revealed through longitudinal genomic surveillance in the Republic of Korea

Kyungmin Park[1,2], Jongwoo Kim[1,3], Seong-Gyu Kim[1,3], Won-Keun Kim[4,5] & Jin-Won Song[1,3]✉

Orthohantavirus hantanense **(HTNV), a major cause of hemorrhagic fever with renal syndrome (HFRS), remains a public health concern in East Asia. We investigated its evolutionary history, reassortment, and genetic diversity by analyzing 123 complete genomes from the Republic of Korea (1976–2023), comprising the most comprehensive dataset to date from this endemic region. Bayesian coalescent analyses estimated evolutionary rates ranging from 1.6 to 6.6 × 10⁻⁴ substitutions per site per year, with the Gn protein exhibiting the highest rate, suggesting gene-specific dynamics. Strong purifying selection (nonsynonymous/synonymous ratio < 0.1) was observed across all segments, reflecting substantial evolutionary constraints. Reassortment analysis revealed frequent segment exchanges, particularly involving the L segment, indicating segment compatibility differences and potential effects on viral fitness. Cline analyses identified a hybrid zone approximately 45 km wide in northern regions, highlighting the role of inter-lineage genetic exchange in enhancing viral diversity and adaptability. These findings clarify the evolution and phylogeography of HTNV and underscore the importance of ongoing genomic surveillance for identifying transmission hotspots, detecting emerging variants, and guiding targeted public health strategies to control endemic HFRS outbreaks effectively.**

Keywords *Orthohantavirus hantanense*, Hemorrhagic fever with renal syndrome, Republic of Korea, Genomic surveillance, Molecular evolution, Reassortment dynamics

Orthohantaviruses, members of the order *Bunyavirales* and family *Hantaviridae*, are enveloped, single-stranded, negative-sense RNA viruses[1]. Their genome comprises large (L), medium (M), and small (S) segments, which encode an RNA-dependent RNA polymerase (RdRp), two surface glycoproteins (Gn and Gc), and a nucleocapsid protein (NP), respectively. These pathogenic viruses cause hemorrhagic fever with renal syndrome (HFRS) in Eurasia and hantavirus cardiopulmonary syndrome in the Americas[2]. Approximately 150,000 HFRS cases are documented annually in East Asia, with fatality rates ranging from < 1–15%[3]. Furthermore, HFRS is primarily associated with infections caused by *Orthohantavirus hantanense* (HTNV), *O. seoulense* (SEOV), *O. puumalaense* (PUUV), and *O. dobravaense* (DOBV)[4]. Transmission to humans occurs predominantly through the inhalation of aerosolized viral particles shed in the saliva, urine, or feces of infected rodents[5].

Phylogeographic inference methods, which incorporate discrete and continuous spatial data, are becoming increasingly prominent in viral phylodynamics. These methods provide crucial insights into viral evolution and the geographic spread of infectious diseases[6]. Phylodynamic analyses of HTNV have revealed significant phylogeographic and epidemiological correlations between patients with HFRS and their rodent reservoir hosts,

[1]Department of Microbiology, Korea University College of Medicine, Goryeodae- ro 73, Seongbuk-gu, Seoul 02841, Republic of Korea. [2]Institute for Viral Diseases, Korea University College of Medicine, Seoul, Republic of Korea. [3]BK21 Graduate Program, Department of Biomedical Sciences, Korea University College of Medicine, Seoul, Republic of Korea. [4]Department of Microbiology, College of Medicine, Hallym University, Chuncheon, Republic of Korea. [5]Institute of Medical Research, College of Medicine, Hallym University, Chuncheon, Republic of Korea. ✉email: jwsong@korea.ac.kr

thereby facilitating the identification of potential viral exposure sites[7]. Further genomic epidemiological studies analyzing nearly full-length HTNV genome sequences from military personnel in the Republic of Korea (ROK) and United States between 2013 and 2015 strengthened these phylogeographic connections[8]. High-resolution phylogeographic associations of HTNV within a 5 km radius were established through active surveillance involving targeted rodent trapping in areas suspected of HFRS outbreaks in 2020, consequently facilitating the identification of infectious agents and potential exposure sites[9]. These high-resolution phylogeographic inference approaches, underpinned by comprehensive viral genome databases, have reconstructed epidemiological linkages between patients and viral sources. Thus, they have substantially contributed to the development of public health interventions for hantavirus-associated diseases.

Segmented RNA viruses can substantially influence molecular evolution through reassortment, which involves the exchange of entire genome segments during co-infection of a host cell by distinct viral strains[10]. This process promotes genome shuffling, increases genetic diversity, and often results in distinct phylogenetic relationships among segments. Reassortment alters critical viral features such as immune evasion, transmissibility, and virulence in humans[11,12]. In viruses such as influenza A and rotavirus A, the reassortment of genetic segments facilitates immune escape and contributes to epidemic outbreaks[12–14]. Similarly, the ongoing reassortment of human immunodeficiency virus results in variants with modified transmissibility and virulence in human populations[15]. Furthermore, the genotype-specific pathogenic potential of the Dabie bandavirus is observed across six pure genotypes and nine reassortants, with varying mortality rates reported in the ROK, China, and Japan[16,17]. Molecular evidence suggests that genetic exchange in HTNV occurs naturally; this contributes to the phylogeographical diversity of the virus in the ROK[18].

A hybrid zone is a geographical area where two distinct taxa that have undergone substantial evolutionary divergence come into contact and interbreed[19]. These regions persist over evolutionary timescales and are characterized by fluctuations in genotype frequencies, manifesting as clines that reflect variations in genetic or phenotypic traits[20]. Their stability is maintained by the delicate interplay between the homogenizing influence of dispersal and the diversifying forces of natural selection[21,22]. Previous studies have documented the existence of hybrid regions between pathogens and their reservoir hosts in natural environments. These zones facilitate genetic diversity and speciation processes, as observed in beak and feather disease viruses and their host species[23]. Hybrid zones are maintained by spatial contact and natural selection pressures in murine cytomegalovirus and its hosts[24]. Genomic surveillance of hybrid zones has revealed noteworthy dynamics, such as the co-circulation of two distinct lineages of *O. tulaense* within a geographical region where different evolutionary clades of the common vole (*Microtus arvalis*) interact and interbreed[25]. More recently, the identification of an HTNV hybrid zone in the ROK suggested that the convergence of divergent genotypes within this area may promote genome reassortment, thereby contributing to enhanced genetic diversity and evolutionary divergence[26].

In this study, we conducted comprehensive genomic surveillance and phylogeographic analyses of HTNV strains collected across the ROK over several decades. We integrated complete genome sequencing, evolutionary analyses, and investigation of genomic reassortment and hybrid zone dynamics to elucidate the mechanisms underlying the genetic diversity and evolution of HTNV. These analyses provide a foundation for the improvement of phylogeographic inference methods, ultimately supporting the development of more effective public health strategies against endemic HFRS outbreaks.

Methods

Establishment of genome database for HTNV

In this study, we obtained all available complete genome sequences of HTNV ($N = 123$) reported in the ROK and their corresponding annotation metadata from National Center for Biotechnology Information (NCBI) GenBank, with data collected until February 28, 2025. When accessible, epidemiological information was gathered to construct detailed datasets, including strain names and origins, lineages, collection dates, reservoir hosts, candidates for genome exchange, accession numbers, and precise geographical locations of trapping sites, encompassing global positioning system (GPS) coordinates, towns, cities, and provinces. Duplicate viral sequences from similar strains and entries with unclear or incomplete information were excluded to ensure metadata accuracy. Similar strains were defined as sequences derived from the same viral isolate that differed only by sequencing method or virus propagation in cell culture. Additionally, sequences with ambiguous collection dates, uncertain host species, imprecise geographic information, or evident sequencing errors were excluded.

Localized Nextstrain build for HTNV in the ROK

In the present study, the Snakemake pipeline for HTNV was employed as a workflow management system to facilitate rapid deployment and ensure the reproducibility of genomic surveillance efforts[27,28]. Geographical data were linked to an extensive metadata set based on GPS coordinates and organized into three resolution levels: 36 towns (denoted as -ri), 11 cities (denoted as -si or -gun), and three provinces. The genomic sequences of each segment were aligned using MAFFT[29]and time-scaled phylogenies were generated using IQ-TREE and TreeTime[30,31]. These phylogenetic trees were then visualized alongside geographic maps, genomic entropy and variations, and frequency panels using the Augur and Auspice toolkits[32].

Evolutionary rate analysis

The HTNV dataset ($N = 123$) encompassing genome sequences reported from 1976 to 2023 includes the L segment encoding the RdRp (6,456 bp), the M segment encoding glycoproteins Gn (1,944 bp) and Gc (1,464 bp), and the S segment encoding the NP (1,290 bp), with all sequences collected for evolutionary rate estimation. Multiple sequence alignments were generated using MAFFT (v7.511)[29]. Evolutionary rates (substitutions per site per year) were inferred using Bayesian Markov chain Monte Carlo (MCMC) analysis implemented in BEAST (v1.10)[33]. The most appropriate nucleotide substitution model was selected using jModelTest2 (v2.1.10),

which identified GTR + G + I as the best-fitting model for all datasets. Temporal calibration was performed based on sampling years, and coalescent analyses were conducted until all parameters reached convergence, with uncertainty assessed using 95% highest posterior density intervals. Effective sample sizes exceeded 200 for all key parameters to ensure statistical robustness. Molecular clock analyses were performed under both strict and relaxed models with an uncorrelated lognormal rate distribution. A range of substitution rate priors was evaluated, and demographic histories were inferred under two models, including constant population size and exponential growth.

Natural selection analysis

The evolutionary pressure acting on the genomes was evaluated by estimating the rate of nonsynonymous (dN) and synonymous (dS) nucleotide substitutions per site per year using the HyPhy software package[34]. Comprehensive natural selection profiles were generated for all genomic segments across complete coding genome datasets to elucidate potential residues under positive or negative selective pressures. Three complementary analytical methods—single-likelihood ancestor counting (SLAC), fixed effects likelihood (FEL), and fast unconstrained Bayesian approximation (FUBAR)—were utilized to determine statistically significant selection sites. These analyses were performed using the Datamonkey Adaptive Evolution Server (https://www.datamonkey.org/; accessed on 18 March 2025)[35]. Statistically robust evidence for positive and negative selection was defined as amino acid positions having p-values < 0.05 (SLAC and FEL) or posterior probability values > 0.9 (FUBAR).

Genetic reassortment analysis

Genetic reassortment was evaluated using the graph incompatibility-based reassortment finder (GiRaF) software[36]. Alignments of the tri-segmented genomes of HTNV were used as inputs for Bayesian inference. One thousand unrooted candidate phylogenetic trees were constructed using the GTR + G + I substitution model, with a burn-in period of 25% (50,000 iterations), and sampling was conducted every 200 iterations. These phylogenies were used to account for evolutionary variability across each genomic segment, adhering to the default parameters set by GiRaF. The confidence threshold was set to 0.7. This procedure was repeated 10 times, resulting in 10 independent MrBayes tree files for each segment.

Cline analysis

Geographic clines were analyzed along one-dimensional transects spanning the contact zones between two distinct HTNV lineages using the HZAR package in R[37]. This software implements functions for the modeling of molecular, genetic or morphological data from hybrid zones, based on classical equilibrium cline models, and utilizes the Metropolis-Hastings MCMC algorithm. The MCMC method was run for one million generations with an initial burn-in of 100,000 iterations for HTNV tripartite genome analysis. The input for cline analysis included information on the spatial separation between localities, genotype distributions, and sample sizes. Hybridization frequencies at the collection sites were visualized, starting from the westernmost point in Paju, Gyeonggi Province, ROK. Genotype frequency data objects were generated using the hzar.doMolecularData1DPops function, and the hzar.plot.obsData function was used to create graphical representations showing both average molecular cline frequencies and typical morphological cline values.

Results

Spatiotemporal genomic surveillance of HTNV in the ROK

High-resolution spatiotemporal surveillance was conducted using complete genomic sequences and epidemiological data from 123 HTNV strains collected in the ROK between 1976 and 2023 (Figs. 1, 2 and 3). Data visualization was filtered based on factors such as strain name, reservoir host, phylogenetic lineage, reassortant candidate, hybrid zone, accession number, collection date, and trapping location. In addition, the resolution was adjusted from the village (36 towns, marked as -ri) to the city (11 cities, marked as -si or -gun) and provincial (three provinces) levels, enabling detailed analysis alongside the phylogenetic data. Lineage 1 of the HTNV tripartite genomes was identified in regions such as Pocheon, Paju, and Yeoncheon in Gyeonggi Province, as well as Chuncheon, Cheorwon, and Hwacheon in Gangwon Province. Lineage 2 spans areas including Yeoncheon in Gyeonggi Province and Chuncheon, Cheorwon, Inje, Hwacheon, and Yanggu in Gangwon Province. Lineage 3 is primarily associated with the southern regions of Gyeonggi Province, including Pocheon, Dongducheon, and Pyeongtaek, and extends to Inje in Gangwon Province. Lineage 4 corresponds to a unique HTNV genetic variant found solely on Jeju Island.

Evolutionary dynamics of HTNV in the ROK

The mean rates of molecular evolution for HTNV, inferred from Bayesian coalescent analyses across multiple molecular clock and demographic models, ranged from 1.6 to 5.1×10^{-4} substitutions per nucleotide per year for RdRp (L segment), 3.3 to 6.6×10^{-4} for Gn, 2.4 to 3.8×10^{-4} for Gc (both M segment), and 2.6 to 3.1×10^{-4} for NP (S segment) (Table 1). Selection pressure analyses indicated that HTNV predominantly underwent purifying selection throughout its evolutionary history, although one positively selected residue (position 547) within the Gn protein was identified using FUBAR (Supplementary Table 1). The estimated dN/dS (ω) ratios were 0.0323, 0.0574, 0.0384, and 0.0322 for RdRp, Gn, Gc, and NP, respectively; the Gn gene exhibited a comparatively higher ω ratio. Additionally, reassortment analyses based on established datasets revealed distinct evolutionary patterns, identifying 33 reassortment events between segments L and M, 44 between L and S, and 18 between M and S (Supplementary Table 2).

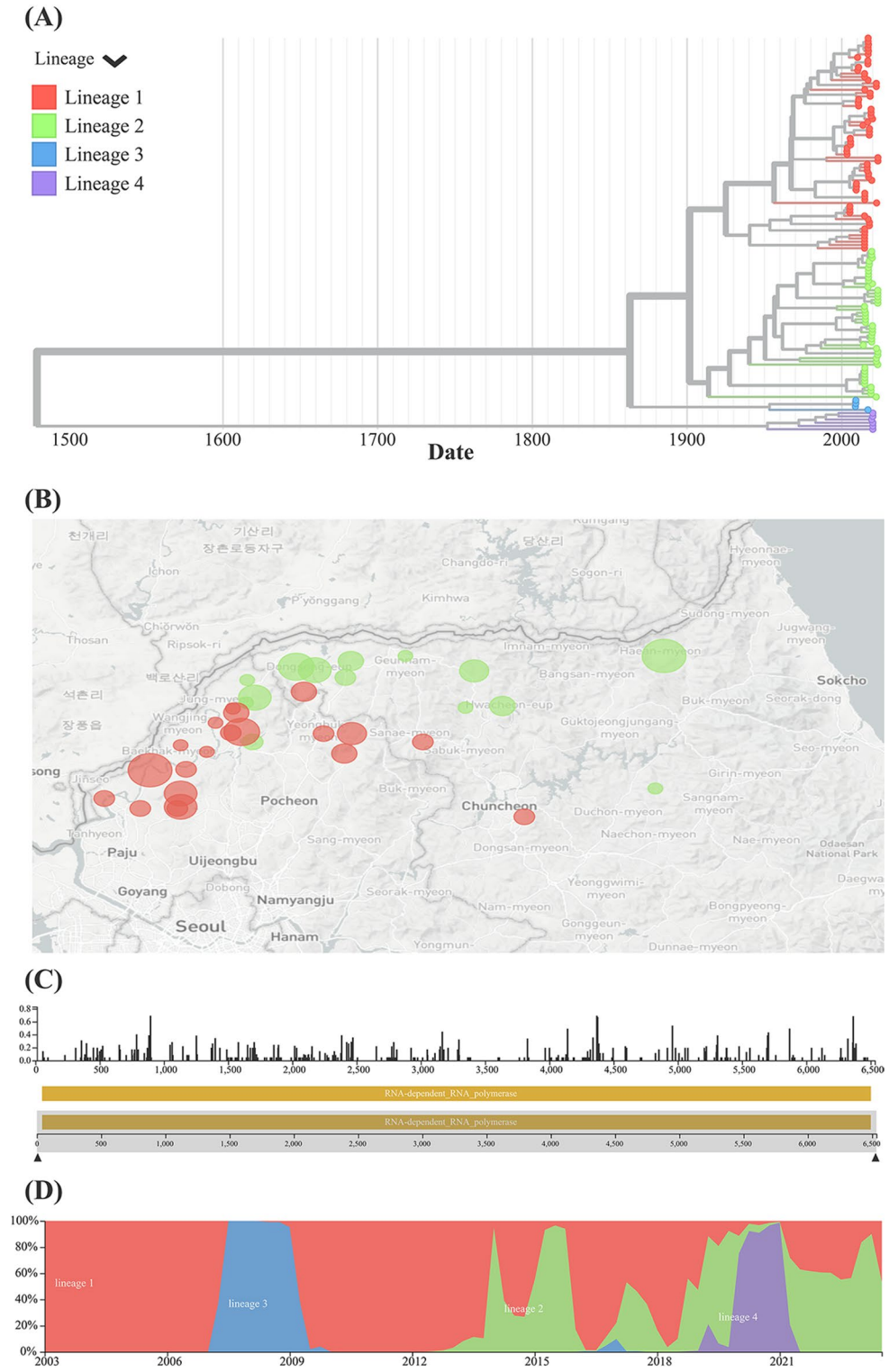

Fig. 1. **Spatiotemporal genomic surveillance of the*Orthohantavirus hantanense*(HTNV) L segment in the Republic of Korea (ROK).** (**A**–**D**) Comprehensive phylodynamic analysis of the HTNV L segment across the ROK between 1976 and 2023. (**A**) A time-scaled phylogenetic tree reconstructed using TimeTree, focusing on the HTNV L segment (positions 1–6,530 nt). (**B**) The geographic distribution of HTNV genomes, with colored circles indicating the population size at each collection site (village level). (**C**) The genomic diversity and entropy within both nucleotide and amino acid sequences of the HTNV L segment. (**D**) The frequency patterns of HTNV lineages circulating in the ROK over the study period, with each lineage in the study denoted by a unique colored symbol.

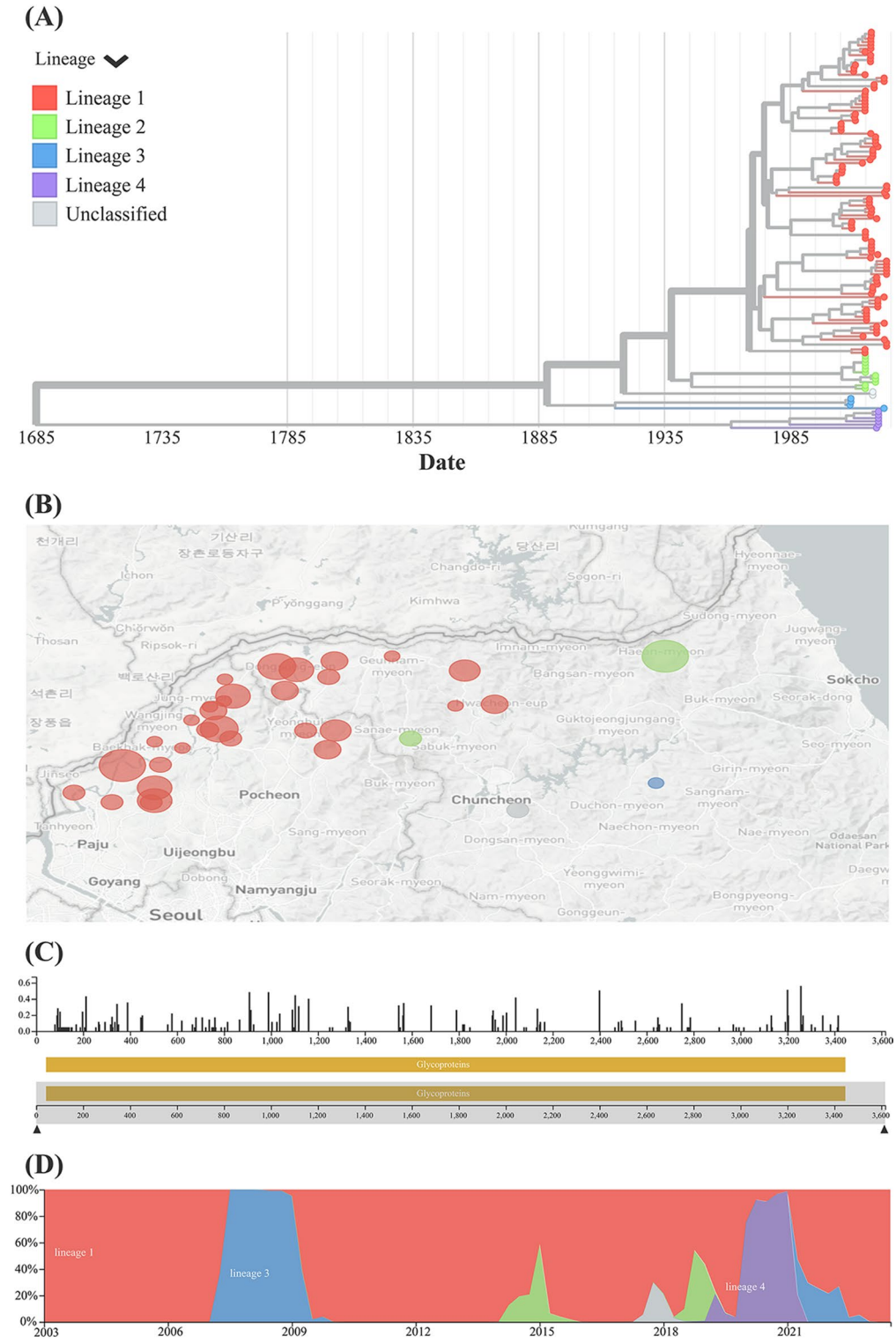

Fig. 2. Spatiotemporal genomic surveillance of the*Orthohantavirus hantanense*(HTNV) M segment in the Republic of Korea (ROK). (**A**–**D**) Comprehensive phylodynamic analysis of the HTNV M segment across the ROK between 1976 and 2023. (**A**) A time-scaled phylogenetic tree reconstructed using TimeTree, focusing on the HTNV M segment (positions 1–3,616 nt). (**B**) The geographic distribution of HTNV genomes, with colored circles indicating the population size at each collection site (village level). (**C**) The genomic diversity and entropy within both nucleotide and amino acid sequences of the HTNV M segment. (**D**) The frequency patterns of HTNV lineages circulating in the ROK over the study period, with each lineage in the study denoted by a unique colored symbol.

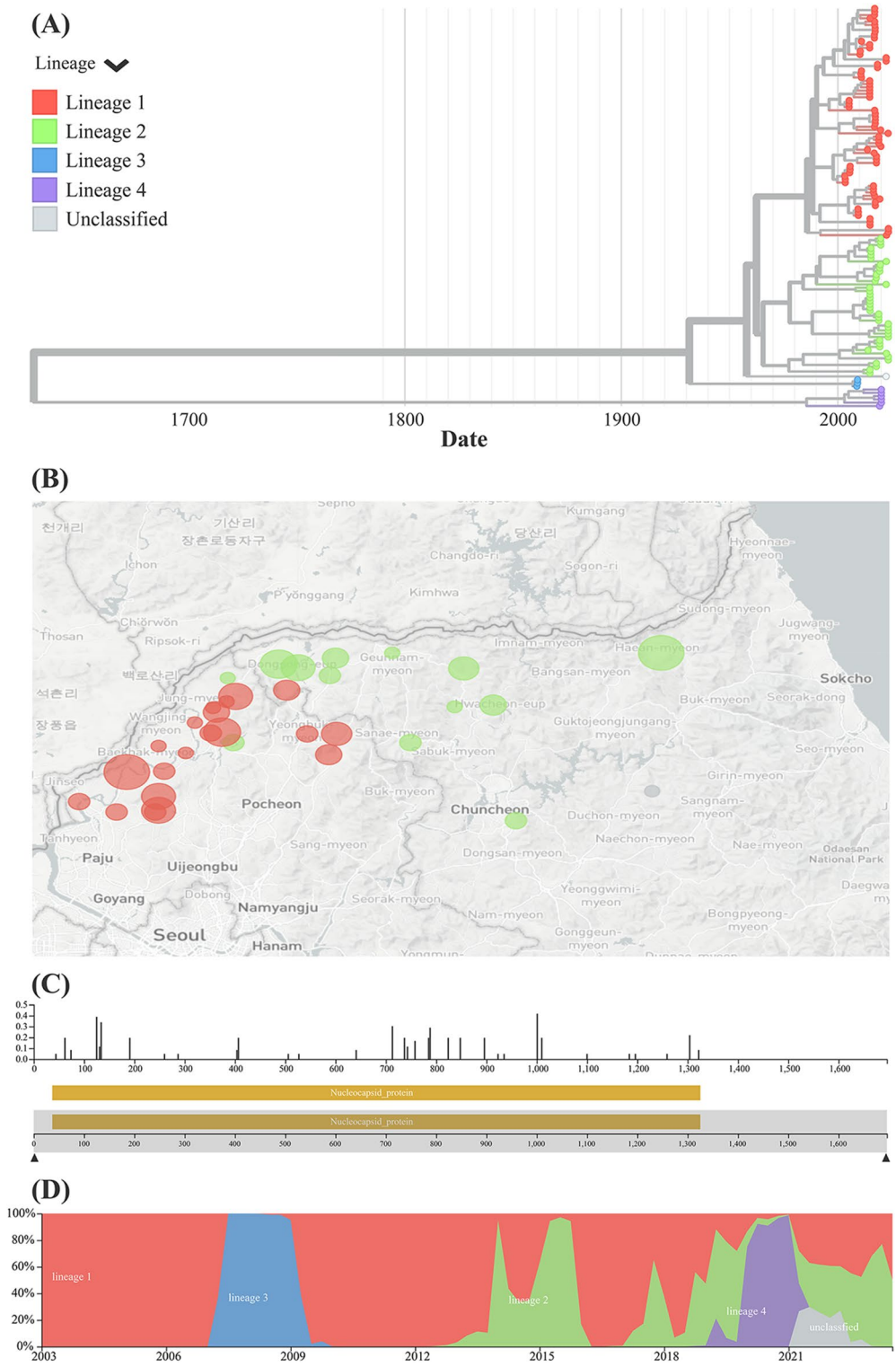

Fig. 3. **Spatiotemporal genomic surveillance of the*Orthohantavirus hantanense*(HTNV) S segment in the Republic of Korea (ROK).** (**A**–**D**) Comprehensive phylodynamic analyses of the HTNV S segment across the ROK between 1976 and 2023. (**A**) A time-scaled phylogenetic tree reconstructed using TimeTree, focusing on the HTNV S segment (positions 1–1,696 nt). (**B**) The geographic distribution of HTNV genomes, with colored circles indicating the population size at each collection site (village level). (**C**) The genomic diversity and entropy within both nucleotide and amino acid sequences of the HTNV S segment. (**D**) The frequency patterns of HTNV lineages circulating in the ROK over the study period, with each lineage in the study denoted by a unique colored symbol.

Segment (gene)	*N*	Sequence length (bp)	Molecular clock	Nucleotide substitutions per site per year (95% HPD)	
				Constant	Exponential
L (RdRp)	123	6,456	Relaxed lognormal	4.6×10^{-4} (2.5×10^{-4} to 7.0×10^{-4})	5.1×10^{-4} (2.8×10^{-4} to 7.9×10^{-4})
			Strict	1.6×10^{-4} (1.1×10^{-4} to 2.2×10^{-4})	1.7×10^{-4} (1.1×10^{-4} to 2.3×10^{-4})
M (Gn)	123	1,944	Relaxed lognormal	6.6×10^{-4} (4.0×10^{-4} to 9.0×10^{-4})	5.5×10^{-4} (3.4×10^{-4} to 7.8×10^{-4})
			Strict	3.3×10^{-4} (2.5×10^{-4} to 4.2×10^{-4})	3.4×10^{-4} (2.5×10^{-4} to 4.3×10^{-4})
M (Gc)	123	1,464	Relaxed lognormal	2.9×10^{-4} (1.6×10^{-4} to 4.3×10^{-4})	3.8×10^{-4} (1.9×10^{-4} to 7.0×10^{-4})
			Strict	2.4×10^{-4} (1.5×10^{-4} to 3.4×10^{-4})	2.4×10^{-4} (1.7×10^{-4} to 3.2×10^{-4})
S (NP)	123	1,290	Relaxed lognormal	2.9×10^{-4} (1.6×10^{-4} to 4.2×10^{-4})	3.1×10^{-4} (1.8×10^{-4} to 4.5×10^{-4})
			Strict	2.6×10^{-4} (1.7×10^{-4} to 3.6×10^{-4})	2.7×10^{-4} (1.8×10^{-4} to 3.6×10^{-4})

Table 1. Bayesian estimates of the rate of nucleotide substitution in *Orthohantavirus Hantanense* collected in the Republic of korea, 1976–2023. HPD, highest posterior density; RdRp, RNA-dependent RNA polymerase; Gn, glycoprotein Gn; Gc, glycoprotein Gc; NP, nucleocapsid protein.

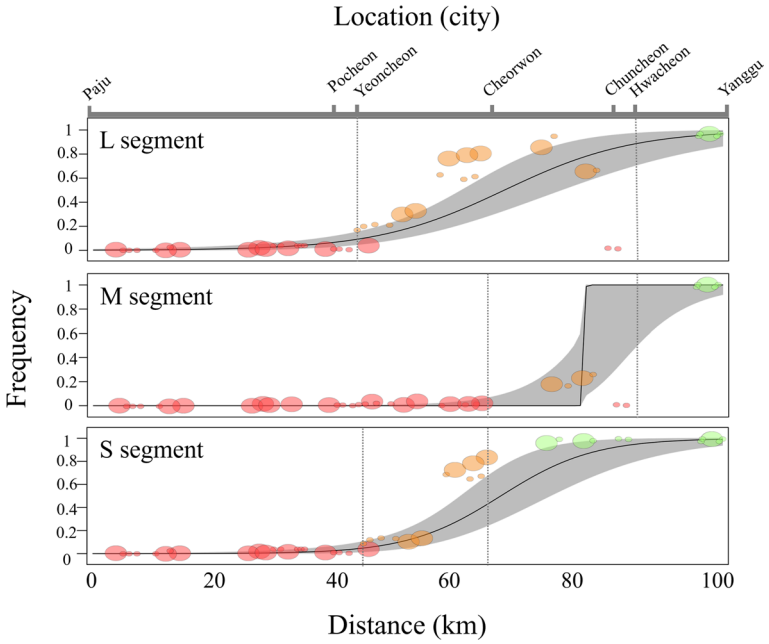

Fig. 4. **Geographic clines and hybrid zone depicting the transition between distinct lineages of*Orthohantavirus hantanense*(HTNV) in the Republic of Korea (ROK).** This figure illustrates the geographic clines and hybrid zone, capturing the transition between different phylogenetic lineages of HTNV across the ROK between 1976 and 2023. The geographic clines reflect estimated shifts in the frequency of genetic traits along a transect extending from the westernmost location in Paju to the easternmost location in Yanggu. For the L segment, a genetic crossbreed area was observed extending from Yeoncheon to Hwacheon (45.3–89.4 km from Paju). The contact region was restricted to Hwacheon (64.3–89.4 km from Paju) in the M segment. The S segment displayed an inter-lineage hybridization zone spanning from Yeoncheon to Cheorwon (45.3–64.3 km from Paju). Symbol sizes represent the number of samples collected, whereas the colors indicate the genotype frequency at each location (red for lineage 1, orange for the hybrid zone, and green for lineage 2). The grey-shaded areas represent regions of 95% credible clines, with dotted lines indicating the boundaries of the hybrid zone.

Analysis of hybrid zones for HTNV in the ROK

Cline analysis revealed shifts in the population frequencies of divergent HTNV lineages 1 and 2 along the geographic transects for each segment. The transition shapes in the L and S segments exhibited spatial homogeneity, whereas the M segment displayed a steeper transition pattern than the others (Fig. 4). Additionally, distinct phylogenetic groups of HTNV in the ROK have specific geographical contact points. A genetic contact zone extending from Yeoncheon to Hwacheon (45.3–89.4 km from Paju) was identified for the L segment. In contrast, the contact area of the M segment was confined to Hwacheon (64.3–89.4 km from Paju). The S segment presented a contact zone stretching from Yeoncheon to Cheorwon (45.3–64.3 km from Paju). The hybrid zone of HTNV spans approximately 45 km (45.3–89.4 km from Paju) and includes areas in Yeoncheon, Gyeonggi Province, as well as Chuncheon, Cheorwon, and Hwacheon in Gangwon Province, ROK (Fig. 5).

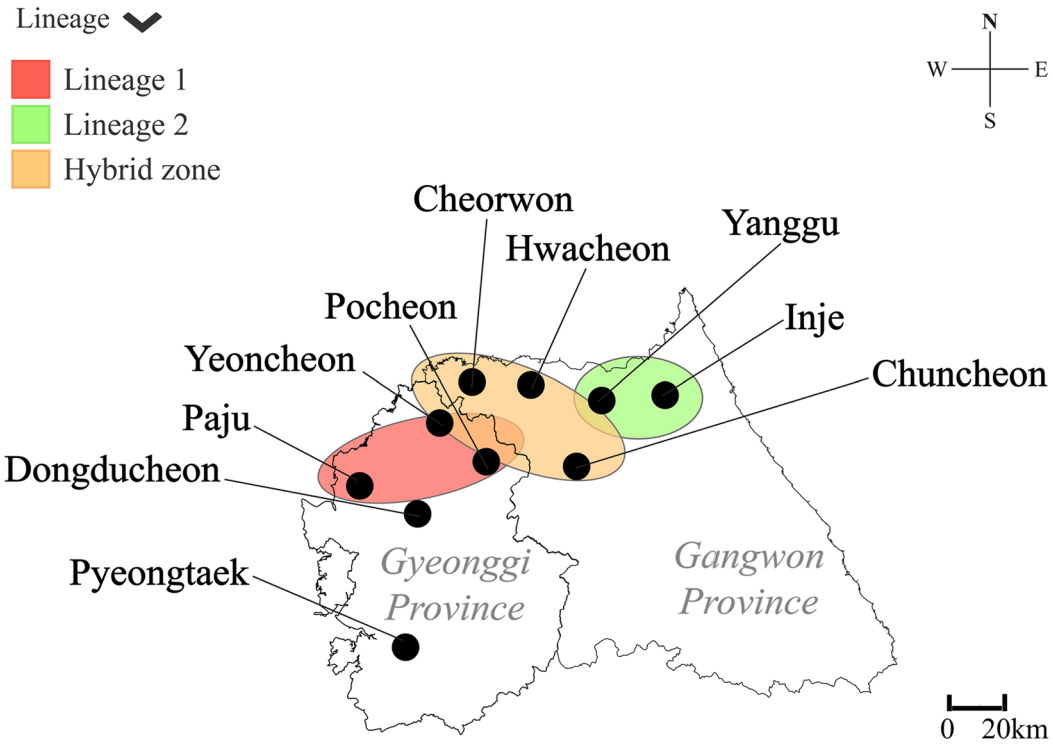

Fig. 5. Geographical locations of the *Orthohantavirus hantanense* (HTNV) hybrid zone in the Republic of Korea (ROK). Two distinct phylogenetic lineages of HTNV intersect within Gyeonggi and Gangwon Provinces, ROK. The hybrid zones are located in four regions: Yeoncheon in Gyeonggi Province, as well as Chuncheon, Cheorwon, and Hwacheon in Gangwon Province. The orange circle highlights the area of geographic overlap between lineage 1 (represented by a red symbol) and lineage 2 (represented by a green symbol) of HTNV. The map was originally generated using Quantum Geographical Information System 3.10 for Mac and later modified using Adobe Illustrator CC 2019.

Discussion

In this study, we analyzed 123 whole-genome sequences of HTNV collected in the ROK between 1976 and 2023, representing the most comprehensive dataset of full-length HTNV genomes from this region to date. Phylogenetic analyses identified four genetic lineages (lineages 1 to 4), each associated with specific geographic clusters within the ROK. Bayesian coalescent analyses, conducted under various molecular clock and demographic models, estimated substitution rates ranging from 1.6 to 6.6×10^{-4} substitutions/site/year across the segments. These values fall within the short-term substitution range of 10^{-2} to 10^{-4} previously reported for rodent-borne hantaviruses and are consistent with patterns observed in other RNA viruses[38,39].

Selective pressure analyses indicated that HTNV strains circulating in the ROK are predominantly subject to purifying selection. All segments exhibited dN/dS ratios below 0.1, reflecting strong evolutionary constraint. The Gn gene displayed the highest dN/dS value (0.0574) and the greatest substitution rate (3.3 to 6.6×10^{-4} substitutions/site/year), indicating a relatively elevated rate of evolution. These findings broadly align with those of Demirev et al., who likewise reported predominant purifying selection in HTNV[40]. However, our analysis consistently revealed higher dN/dS ratios across all segments compared to their study, suggesting that HTNV strains in the ROK may be under slightly stronger evolutionary pressures, potentially shaped by region-specific factors. Additionally, we identified a single codon under positive selection (residue 547) in the Gn gene. This site is located within the short C-terminal cytoplasmic tail (CT), a functionally important region involved in several critical steps of the viral life cycle[41]. The CT interacts with the NP and ribonucleocapsid complexes, likely serving as a structural bridge between internal viral components and the glycoprotein lattice[42]. It also contains a conserved ββα-type zinc finger domain essential for NP binding, and its distal region is implicated in nonspecific RNA binding[43]. Although the identification of a positively selected site in this functionally relevant region is noteworthy, the signal was detected using a single method and should be interpreted with caution. Further investigation is warranted to assess whether this substitution affects virion morphogenesis, intracellular trafficking, or host-specific adaptation.

Previous studies have shown that genome exchange among hantaviruses typically occurs within or between closely related lineages[44,45]. Among the three segments, the M segment has most frequently been implicated in reassortment, likely due to its functional plasticity and potential to confer adaptive advantages[46]. For instance, reassortment involving the M segment has been documented for *O. sinnombreense* and *O. andesense* in both natural and experimental settings, often resulting in geographically structured clades[47–49]. Experimental reassortment has also been observed in DOBV, again primarily affecting the M segment[50]. In contrast,

reassortment involving the L or S segments has been reported in HTNV, SEOV, and PUUV[8,40,51]. In our analysis, which focused exclusively on HTNV genomes sampled within the ROK, we identified a different pattern: reassortment was more frequently observed in the L segment than in the M or S segments. Although L segment reassortment has been previously reported in HTNV[52,53]its relative prominence in our dataset merits further attention. Reassortment events involving the L segment were especially common in strains from Paju, Gyeonggi Province, suggesting possible regional variation in segment exchange dynamics. However, we cannot exclude the possibility that uneven sampling intensity contributed to this observed pattern. As with other segmented RNA viruses, successful reassortment in HTNV is likely constrained by the need to preserve packaging signal compatibility and RNA–protein interactions[10]. Whether L segment exchange confers functional advantages—such as enhanced replication, transmission efficiency, or host adaptability—remains unresolved.

Approximately 400 cases of HFRS are reported annually in the ROK, with a mortality rate of 1–4% (accessible online at https://dportal.kdca.go.kr/pot/is/rginEDW.do). HTNV is the primary etiological agent and is particularly prevalent in the northern regions of the Gyeonggi and Gangwon Provinces, affecting both military personnel and civilians[18,53–55]. In the present study, we identified a hybrid zone spanning approximately 45 km, covering four key locations: Yeoncheon in Gyeonggi Province and Chuncheon, Cheorwon, and Hwacheon in Gangwon Province. Compared to previous findings from 2020, the expansion of contact areas in Yeoncheon and Chuncheon effectively doubles the previously documented extent of the hybrid zone[26]potentially reflecting increased opportunities for genome exchange. We also observed distinct cline patterns among the HTNV L, M, and S segments, suggesting varying tendencies for reassortment and hybrid zone expansion. The L segment exhibited the broadest cross-lineage distribution, consistent with its higher exchange frequency, whereas the M segment appeared more compatible with lineage 1 within the hybrid zone. These patterns may be shaped by differences in local viral fitness or segment-specific functional constraints. According to evolutionary theory, contact zones are expected to favor genotypes with higher relative fitness[46,56]which may contribute to the observed segment dynamics.

Although ecological and demographic variables were not directly examined in this study, previous research has demonstrated that urbanization, human migration, rodent population dynamics, and environmental or climatic changes can influence the spatial and temporal patterns of hantavirus transmission[57,58]. For instance, long-term surveillance in China has shown associations between rural-to-urban migration and sustained hantavirus epidemics, highlighting the importance of socio-environmental drivers in shaping virus–host interactions[59]. While such external factors may not fully account for the hybrid zone expansion observed in our dataset, they provide a meaningful context for interpreting the ecological and epidemiological mechanisms underlying our findings. Future research integrating viral genomic data with ecological and demographic information will be essential to evaluate their roles in hybrid zone dynamics and viral emergence.

This report highlights several limitations that warrant further exploration: (1) the insufficient availability of genomic sequences and epidemiological data from other endemic areas in the ROK, especially in the southern regions; (2) the uncertain biological advantages associated with HTNV L segment exchange, specifically regarding its impact on viral replication and pathogenicity; and (3) the need for more in-depth research on the implications of hybrid zone expansion, which may lead to alterations that could influence pathogenicity in humans.

In conclusion, this study provides the most comprehensive whole-genome analysis of HTNV in the ROK to date, revealing four distinct genetic lineages with clear regional clustering and a notable concentration of reassortment events in the L segment. Purifying selection was the dominant evolutionary force across all segments, with relatively elevated rates and a single positively selected site detected in the Gn gene. The identification of an expanded hybrid zone and segment-specific cline patterns suggests active genome exchange dynamics in northern regions. These insights not only enhance our understanding of HTNV evolution but may also inform regionally tailored genomic surveillance strategies, support the development of more sensitive molecular diagnostics, and assist in prioritizing public health responses in areas with heightened reassortment potential.

Data availability

The datasets generated during and/or analysed during the current study are available from the corresponding author on reasonable request.

Received: 2 June 2025; Accepted: 7 July 2025
Published online: 09 July 2025

References

1. Vaheri, A. et al. Hantavirus infections in Europe and their impact on public health. *Rev. Med. Virol.* **23**, 35–49 (2013).
2. Kruger, D. H., Figueiredo, L. T., Song, J. W. & Klempa, B. Hantaviruses–globally emerging pathogens. *J. Clin. Virol.* **64**, 128–136 (2015).
3. Jonsson, C. B., Figueiredo, L. T. & Vapalahti, O. A global perspective on hantavirus ecology, epidemiology, and disease. *Clin. Microbiol. Rev.* **23**, 412–441 (2010).
4. Kim, W. K. et al. Genomic epidemiology and active surveillance to investigate outbreaks of hantaviruses. *Front. Cell. Infect. Microbiol.* **10**, 532388. https://doi.org/10.3389/fcimb.2020.532388 (2020).
5. Forbes, K. M., Sironen, T. & Plyusnin, A. Hantavirus maintenance and transmission in reservoir host populations. *Curr. Opin. Virol.* **28**, 1–6 (2018).
6. Grenfell, B. T. et al. Unifying the epidemiological and evolutionary dynamics of pathogens. *Science* **303**, 327–332 (2004).
7. Song, J. W. et al. Hemorrhagic fever with renal syndrome in 4 US soldiers, South korea, 2005. *Emerg. Infect. Dis.* **15**, 1833–1836 (2009).

8. Kim, W. K. et al. Phylogeographic analysis of hemorrhagic fever with renal syndrome patients using multiplex PCR-based next generation sequencing. *Sci. Rep.* **6**, 26017. https://doi.org/10.1038/srep26017 (2016).
9. Kim, W. K. et al. Active targeted surveillance to identify sites of emergence of hantavirus. *Clin. Infect. Dis.* **70**, 464–473 (2020).
10. McDonald, S. M., Nelson, M. I., Turner, P. E. & Patton, J. T. Reassortment in segmented RNA viruses: mechanisms and outcomes. *Nat. Rev. Microbiol.* **14**, 448–460 (2016).
11. Vijaykrishna, D., Mukerji, R. & Smith, G. J. RNA virus reassortment: an evolutionary mechanism for host jumps and immune evasion. *PLoS Pathog.* **11**, e1004902. https://doi.org/10.1371/journal.ppat.1004902 (2015).
12. Iturriza-Gómara, M., Isherwood, B., Desselberger, U. & Gray, J. Reassortment in vivo: driving force for diversity of human rotavirus strains isolated in the united Kingdom between 1995 and 1999. *J. Virol.* **75**, 3696–3705 (2001).
13. Horimoto, T. & Kawaoka, Y. Influenza: lessons from past pandemics, warnings from current incidents. *Nat. Rev. Microbiol.* **3**, 591–600 (2005).
14. McDonald, S. M. et al. Evolutionary dynamics of human rotaviruses: balancing reassortment with preferred genome constellations. *PLoS Pathog.* **5**, e1000634. https://doi.org/10.1371/journal.ppat.1000634 (2009).
15. Vijaykrishna, D. et al. Reassortment of pandemic H1N1/2009 influenza A virus in swine. *Science* **328**, 1529 (2010).
16. Yun, S. M. et al. Genetic and pathogenic diversity of severe fever with thrombocytopenia syndrome virus (SFTSV) in South Korea. *JCI Insight.* **5**, e129531. https://doi.org/10.1172/jci.insight.129531 (2020).
17. Fu, Y. et al. Phylogeographic analysis of severe fever with thrombocytopenia syndrome virus from Zhoushan islands, china: implication for transmission across the ocean. *Sci. Rep.* **6**, 19563. https://doi.org/10.1038/srep19563 (2016).
18. Kim, J. A. et al. Genetic diversity and reassortment of Hantaan virus tripartite RNA genomes in nature, the Republic of Korea. *PLoS Negl. Trop. Dis.* **10**, e0004650. https://doi.org/10.1371/journal.pntd.0004650 (2016).
19. Barton, N. H. & Hewitt, G. M. Adaptation, speciation and hybrid zones. *Nature* **341**, 497–503 (1989).
20. Endler, J. A. Geographic variation, speciation, and clines. *Monogr. Popul. Biol.* **10**, 1–246 (1977).
21. Slatkin, M. Gene flow and selection in a Cline. *Genetics* **75**, 733–756 (1973).
22. Barton, N. H. & Hewitt, G. M. Analysis of hybrid zones. *Annu. Rev. Ecol. Syst.* **16**, 113–148 (1985).
23. Eastwood, J. R. et al. Phylogenetic analysis of beak and feather disease virus across a host ring-species complex. *Proc. Natl. Acad. Sci. U S A.* **111**, 14153–14158 (2014).
24. Goüy de Bellocq, J., Baird, S. J., Albrechtová, J., Sobeková, K. & Piálek, J. Murine cytomegalovirus is not restricted to the house mouse *Mus musculus* domesticus: prevalence and genetic diversity in the European house mouse hybrid zone. *J. Virol.* **89**, 406–414 (2015).
25. Saxenhofer, M., Schmidt, S., Ulrich, R. G. & Heckel, G. Secondary contact between diverged host lineages entails ecological speciation in a European hantavirus. *PLoS Biol.* **17**, e3000142. https://doi.org/10.1371/journal.pbio.3000142 (2019).
26. Lee, G. Y. et al. Phylogeographic diversity and hybrid zone of *Hantaan orthohantavirus* collected in Gangwon province, Republic of Korea. *PLoS Negl. Trop. Dis.* **14**, e0008714. https://doi.org/10.1371/journal.pntd.0008714 (2020).
27. Koster, J. & Rahmann, S. Snakemake–a scalable bioinformatics workflow engine. *Bioinformatics* **28**, 2520–2522 (2012).
28. Park, K. et al. Web visualization for Spatiotemporal genomic epidemiology, annotation, and mutation dynamics of *Orthohantavirus Hantanense* using nextstrain. *Am. J. Trop. Med. Hyg.* **112**, 871–874 (2025).
29. Katoh, K., Misawa, K., Kuma, K. & Miyata, T. MAFFT: a novel method for rapid multiple sequence alignment based on fast fourier transform. *Nucleic Acids Res.* **30**, 3059–3066 (2002).
30. Nguyen, L. T., Schmidt, H. A., von Haeseler, A. & Minh, B. Q. IQ-TREE: a fast and effective stochastic algorithm for estimating maximum-likelihood phylogenies. *Mol. Biol. Evol.* **32**, 268–274 (2015).
31. Sagulenko, P., Puller, V., Neher, R. A. & TreeTime Maximum-likelihood phylodynamic analysis. *Virus Evol.* **4**, vex042. https://doi.org/10.1093/ve/vex042 (2018).
32. Hadfield, J. et al. Nextstrain: real-time tracking of pathogen evolution. *Bioinformatics* **34**, 4121–4123 (2018).
33. Suchard, M. A. et al. Bayesian phylogenetic and phylodynamic data integration using BEAST 1.10. *Virus Evol.* **4** (vey016). https://doi.org/10.1093/ve/vey016 (2018).
34. Kosakovsky Pond, S. L. et al. HyPhy 2.5-A customizable platform for evolutionary hypothesis testing using phylogenies. *Mol. Biol. Evol.* **37**, 295–299 (2020).
35. Weaver, S. et al. Datamonkey 2.0: a modern web application for characterizing selective and other evolutionary processes. *Mol. Biol. Evol.* **35**, 773–777 (2018).
36. Nagarajan, N. & Kingsford, C. GiRaF: robust, computational identification of influenza reassortments via graph mining. *Nucleic Acids Res.* **39**, e34. https://doi.org/10.1093/nar/gkq1232 (2011).
37. Derryberry, E. P., Derryberry, G. E., Maley, J. M. & Brumfield, R. T. HZAR: hybrid zone analysis using an R software package. *Mol. Ecol. Resour.* **14**, 652–663 (2014).
38. Ramsden, C. et al. High rates of molecular evolution in hantaviruses. *Mol. Biol. Evol.* **25**, 1488–1492 (2008).
39. Jenkins, G. M., Rambaut, A., Pybus, O. G. & Holmes, E. C. Rates of molecular evolution in RNA viruses: a quantitative phylogenetic analysis. *J. Mol. Evol.* **54**, 156–165 (2002).
40. Demirev, A. V. et al. Exploring the genetic diversity and molecular evolution of Seoul and Hantaan orthohantaviruses. *Viruses* **16**, 105. https://doi.org/10.3390/v16010105 (2024).
41. Serris, A. et al. The Hantavirus Surface Glycoprotein Lattice and Its Fusion Control Mechanism. *Cell* 183, 442–456 e416; (2020). https://doi.org/10.1016/j.cell.2020.08.023
42. Hepojoki, J. et al. Cytoplasmic Tails of hantavirus glycoproteins interact with the nucleocapsid protein. *J. Gen. Virol.* **91**, 2341–2350 (2010).
43. Cifuentes-Munoz, N., Salazar-Quiroz, N. & Tischler, N. D. Hantavirus Gn and Gc envelope glycoproteins: key structural units for virus cell entry and virus assembly. *Viruses* **6**, 1801–1822 (2014).
44. Razzauti, M., Plyusnina, A., Sironen, T., Henttonen, H. & Plyusnin, A. Analysis of puumala hantavirus in a bank vole population in Northern finland: evidence for co-circulation of two genetic lineages and frequent reassortment between strains. *J. Gen. Virol.* **90**, 1923–1931 (2009).
45. Lee, S. H. et al. Dynamic circulation and genetic exchange of a Shrew-borne hantavirus, Imjin virus, in the Republic of Korea. *Sci. Rep.* **7**, 44369. https://doi.org/10.1038/srep44369 (2017).
46. Klempa, B. Reassortment events in the evolution of hantaviruses. *Virus Genes.* **54**, 638–646 (2018).
47. Henderson, W. W. et al. Naturally occurring sin Nombre virus genetic reassortants. *Virology* **214**, 602–610 (1995).
48. Rodriguez, L. L., Owens, J. H., Peters, C. J. & Nichol, S. T. Genetic reassortment among viruses causing hantavirus pulmonary syndrome. *Virology* **242**, 99–106 (1998).
49. Padula, P. J. et al. Genetic diversity, distribution, and serological features of hantavirus infection in five countries in South America. *J. Clin. Microbiol.* **38**, 3029–3035 (2000).
50. Kirsanovs, S. et al. Genetic reassortment between high-virulent and low-virulent Dobrava-Belgrade virus strains. *Virus Genes.* **41**, 319–328 (2010).
51. Razzauti, M., Plyusnina, A., Henttonen, H. & Plyusnin, A. Accumulation of point mutations and reassortment of genomic RNA segments are involved in the microevolution of puumala hantavirus in a bank vole (*Myodes glareolus*) population. *J. Gen. Virol.* **89**, 1649–1660 (2008).
52. Park, K. et al. Epidemiological surveillance and phylogenetic diversity of *Orthohantavirus Hantanense* using high-fidelity nanopore sequencing, Republic of Korea. *PLoS Negl. Trop. Dis.* **19**, e0012859. https://doi.org/10.1371/journal.pntd.0012859 (2025).

53. Cho, S. et al. Urinary genome detection and tracking of Hantaan virus from hemorrhagic fever with renal syndrome patients using multiplex PCR-based next-generation sequencing. *PLoS Negl. Trop. Dis.* **15**, e0009707. https://doi.org/10.1371/journal.pntd.0009707 (2021).
54. Park, K. et al. Multiplex PCR-Based nanopore sequencing and epidemiological surveillance of *Hantaan orthohantavirus* in *Apodemus agrarius*, Republic of Korea. *Viruses* **13**, 847. https://doi.org/10.3390/v13050847 (2021).
55. Kim, J. et al. High-resolution phylogeographical surveillance of *Hantaan orthohantavirus* using rapid amplicon-based flongle sequencing, Republic of Korea. *J. Med. Virol.* **96**, e29346. https://doi.org/10.1002/jmv.29346 (2024).
56. Drewes, S. et al. Host-Associated absence of human puumala virus infections in Northern and Eastern Germany. *Emerg. Infect. Dis.* **23**, 83–86 (2017).
57. Kallio, E. R. et al. Cyclic hantavirus epidemics in humans–predicted by rodent host dynamics. *Epidemics* **1**, 101–107 (2009).
58. Tian, H. & Stenseth, N. C. The ecological dynamics of hantavirus diseases: from environmental variability to disease prevention largely based on data from China. *PLoS Negl. Trop. Dis.* **13**, e0006901. https://doi.org/10.1371/journal.pntd.0006901 (2019).
59. Tian, H. et al. Urbanization prolongs hantavirus epidemics in cities. *Proc. Natl. Acad. Sci. U S A.* **115**, 4707–4712 (2018).

Acknowledgements

This study was supported by the Agency for Defense Development (UE242006TD and 411FF5-912A01201). The funders had no role in the study design, data collection and analysis, decision to publish, or manuscript preparation.

Author contributions

K.P. designed the study, analyzed and interpreted data, and wrote the manuscript. J.K. and S.-G.K., and W.-K.K. provided scientific discussion. J.-W.S. supervised the study, analyzed and interpreted data, and reviewed the manuscript.

Declarations

Competing interests

The authors declare no competing interests.

Additional information

Supplementary Information The online version contains supplementary material available at https://doi.org/10.1038/s41598-025-11003-z.

Correspondence and requests for materials should be addressed to J.-W.S.